

Mitral Annular Size Predicts Alfieri Stitch Tension in Mitral Edge-to-Edge Repair

Tomasz A. Timek^{1,6}, Sten L. Nielsen⁴, David T. Lai¹, Frederick Tibayan¹, David Liang², George T. Daughters^{1,5}, Philip Beineke³, Trevor Hastie³, Neil B. Ingels, Jr.^{1,5}, D. Craig Miller¹

¹Department of Cardiothoracic Surgery, ²Division of Cardiovascular Medicine, ³Department of Biostatistics, Stanford University School of Medicine, Stanford, CA, USA, ⁴Department of Cardiothoracic and Vascular Surgery, Aarhus University, Aarhus, Denmark, ⁵Laboratory of Cardiovascular Physiology and Biophysics, Research Institute of the Palo Alto Medical Foundation, Palo Alto, CA, USA

⁶Present address: Department of Surgery, Loma Linda University Medical Center, Loma Linda, CA, USA

Background and aim of the study: Whilst increased 'Alfieri stitch' tension may reduce the durability of 'edge-to-edge' mitral repair, the factors affecting suture tension are unknown. In order to study hemodynamics and left ventricular (LV) and annular dynamics that determine suture tension, the central edge of the mitral leaflets was approximated with a miniature force transducer to measure leaflet tension (T) at the leaflet approximation point.

Methods: Eight sheep were studied under open-chest conditions immediately after surgical placement of a force transducer and implantation of radiopaque markers on the left ventricle and mitral annulus (MA). Hemodynamic variables were altered by two caval occlusion steps ($\Delta V1$ and $\Delta V2$) and dobutamine infusion. Three-dimensional marker coordinates were obtained by simultaneous biplane videofluoroscopy to measure LV volume, MA area (MAA) and septal-lateral (SL) annular dimension throughout the cardiac cycle.

Results: At baseline, peak Alfieri stitch tension (0.30 ± 0.18 N) was observed 96 ± 61 ms prior to end-dias-

tole coincident with peak annular SL diameter (98 ± 58 ms before end-diastole). Dobutamine infusion decreased suture tension (from 0.30 ± 0.18 N to 0.20 ± 0.12 N, $p = 0.01$), although peak systolic pressure increased significantly (138 ± 19 versus 115 ± 14 mmHg; $p = 0.03$). A regression model was fitted with the goal of interpreting the hemodynamic and geometric predictors of tension as their influence varied with time: Tt (N) = $0.1916 + 0.2115 \times SL$ (cm) - $0.1996 \times MAA/SL$ (cm²/cm) + $ft \times LVP$ (mmHg), where Tt is tension at any time during the cardiac cycle and ft is the time-varying coefficient of LVP.

Conclusion: Tension on the leaflets in the edge-to-edge repair is determined primarily by MA SL size, and paradoxically is lower when the contractile state is enhanced. This indicates that annular and/or LV dilatation increase stitch tension and may adversely affect durability of the repair if concomitant ring annuloplasty is not performed.

The Journal of Heart Valve Disease 2004;13:165-173

Mitral valve repair restores mitral competency in most patients with mitral regurgitation (1,2), and improves clinical outcome relative to mitral valve replacement (3). Surgical techniques continue to evolve to encompass a wider spectrum of mitral pathology to offer mitral repair to more patients (4-8). A novel method, the edge-to-edge mitral repair, has been added by Alfieri and colleagues (9). This technique is simple, and customized such that leaflet approximation is performed at the location of the regurgitant jet (10). The edge-to-edge repair is effective in correcting mitral insufficiency of varying etiology

(10-12), including ischemic heart disease (13) and end-stage cardiomyopathy (14,15). This procedure can be used to address mitral lesions involving leaflet prolapse or leaflet restriction expediently (10), and provides predictable mid-term results for certain mitral lesions (12).

The durability of the Alfieri repair remains a concern however, as long-term follow up is not yet available. It is intuitive that increased Alfieri stitch tension may reduce durability of the edge-to-edge mitral repair and lead to recurrent mitral regurgitation, but the determinants of tension at the leaflet approximation point are unknown. In order to identify possible variables affecting stitch tension, a miniature force transducer was implanted to approximate the mitral leaflets, as in the edge-to-edge repair, to measure Alfieri stitch tension throughout the cardiac cycle under varying hemodynamic conditions.

Address for correspondence:

D. Craig Miller MD, Department of Cardiothoracic Surgery, Falk Cardiovascular Research Center, Stanford University School of Medicine, Stanford, California 94305-5247, USA
e-mail: dcm@stanford.edu

Materials and methods

Surgical preparation

The general procedures used have been described previously (16). Sub-epicardial miniature radiopaque markers were inserted into the left ventricle of eight adult male castrated sheep (mean body weight 68 ± 5 kg), along four equally spaced longitudinal meridians at two levels between the left ventricular (LV) apex and the base (Fig. 1A). Following the establishment of cardiopulmonary bypass (CPB) and cardioplegic arrest, eight additional markers were sutured around the circumference of the mitral annulus (MA). Subsequently, the centers of the anterior and posterior mitral leaflets were approximated at their edges with a 5-0 polypropylene suture reinforced with two small Teflon-felt pledgets, thus creating a 'double-orifice' mitral valve (Fig. 1B). The approximating suture or Alfieri stitch was placed approximately 5 mm from each leaflet edge, and also secured a miniature force transducer (Fig. 2), which served as another radiopaque marker. The force transducer was constructed of a slit copper ring, 5 mm in diameter and 0.4 mm thick. On each side of the slit, two small holes were used for suture attachment. Technical specifications of the transducer have been described previously (17). Two pneumatic occluders used for sudden volume reduction were placed around the superior and inferior vena cava and externalized. A micromanometer pressure transducer (PA4.5-X6; Konigsberg Instruments, Inc., Pasadena, CA, USA) was placed in the LV chamber through the apex.

Following completion of marker implantation, the heart was defibrillated, and each animal weaned from CPB and transferred immediately to the experimental animal catheterization laboratory where they were studied intubated, open-chest, and anesthetized with ketamine (1-4 mg/kg/h, intravenous infusion) and diazepam (5 mg intravenous bolus as needed). Intravenous esmolol (20-50 $\mu\text{g}/\text{kg}/\text{min}$) was infused to minimize reflex sympathetic responses. Simultaneous biplane videofluoroscopy, hemodynamic data recordings, and force transducer tension readings were measured under four experimental conditions: Baseline, two consecutive steps of volume reduction (ΔV_1 and ΔV_2) using the pneumatic occluders, and during inotropic stimulation with dobutamine (10 $\mu\text{g}/\text{kg}/\text{min}$).

All animals received humane care in compliance with the *Principles of Laboratory Animal Care* formulated by the National Society for Medical Research and the *Guide for Care and Use of Laboratory Animals* prepared by the National Academy of Sciences and published by the National Institutes of Health (DHEW NIHG publication 85-23, revised 1985). This study was approved

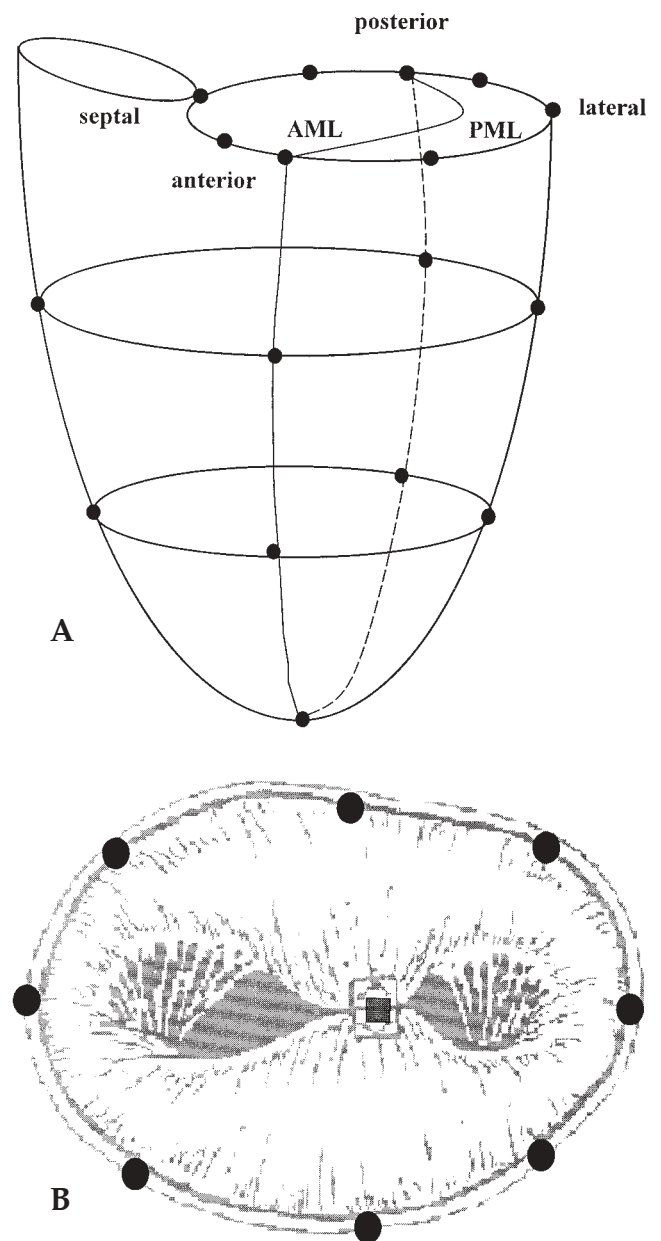


Figure 1: A) Miniature radiopaque marker array (solid circles are myocardial markers) implanted in the left ventricle and mitral annulus in this experimental study. AML: Anterior mitral leaflet; PML: Posterior mitral leaflet. B) Diagram of the mitral valve after the edge-to-edge mitral repair. Solid circles represent mitral annular markers ($n = 8$), with the force transducer approximating the leaflets represented by the solid square in the middle of the valve.

by the Stanford Medical Center Laboratory Research Animal Review committee and conducted according to Stanford University policy.

Data acquisition

Images were acquired with the animal in the right lateral decubitus position and with the chest open, using a Philips Optimus 2000 biplane Lateral ARC 2/Poly DIAGNOST C2 system (Philips Medical Systems, North America Company, Pleasanton, CA, USA) with the image intensifier in the 9-inch (20-cm) fluoroscopic mode. Data from the two radiographic views were digitized and merged using custom-designed software (18) to yield the three-dimensional (3-D) *x*, *y*, *z* coordinates for each of the radiopaque markers every 16.7 ms throughout the cardiac cycle. Force transducer tension, ascending aortic pressure, LV pressure and ECG voltage signals were also digitized and recorded simultaneously.

Data analysis

Two to three consecutive steady-state beats during baseline, the two occlusion steps, and after dobutamine infusion were averaged and defined as 'Baseline', ' ΔV_1 ', ' ΔV_2 ' and 'dobutamine' data for each animal. During each cardiac cycle, end-systole (ES) was defined as the frame containing peak rate of LV pressure fall ($-dP/dt$); end-diastole (ED) was defined as the videofluoroscopic frame containing the peak of the ECG R-wave. Instantaneous LV volume was computed from the epicardial LV markers as described previously (19). Stroke volume was calculated as the difference between LV end-diastolic volume (EDV) and LV end-systolic volume (ESV).

Mitral annular dynamics

Mitral annular area (MAA) was computed from the 3-D coordinates of the eight markers sutured to the

mitral annulus using an annular centroid. The septal-lateral (SL) annular diameter was calculated as the distance in 3-D space between markers placed on the mid-anterior and mid-posterior mitral annulus. Commissure-commissure annular diameter was calculated as the distance between the commissural markers.

Statistical analysis

All data were reported as mean \pm SD, unless otherwise indicated. Hemodynamic and marker-derived data from consecutive steady-state beats from each heart were time-aligned at end-diastole. Marker data were calculated over 20 frames before and after end-diastole, thus allowing evaluation over a time period of 650 ms. The mean (\pm SD) for each variable at each sampling instant was computed for Control, ΔV_1 , ΔV_2 and dobutamine conditions. Data were compared using Student's *t*-test for paired comparisons and repeated measures ANOVA when appropriate.

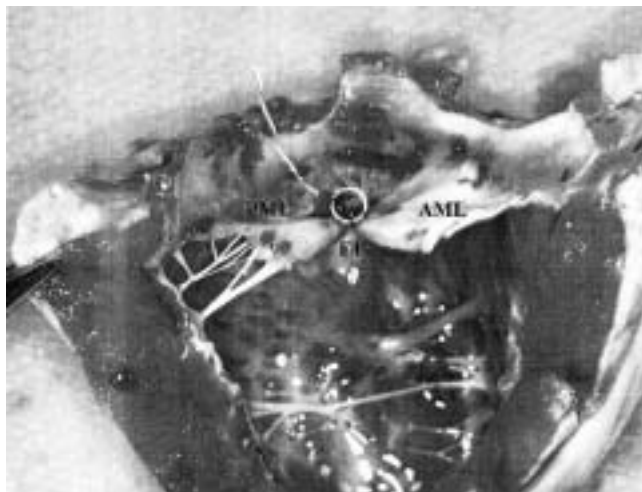


Figure 2: Post-mortem ex-vivo sagittal section of the heart of one of the study animals showing the C-shaped miniature force transducer (FT) between the anterior (AML) and posterior (PML) mitral leaflets.

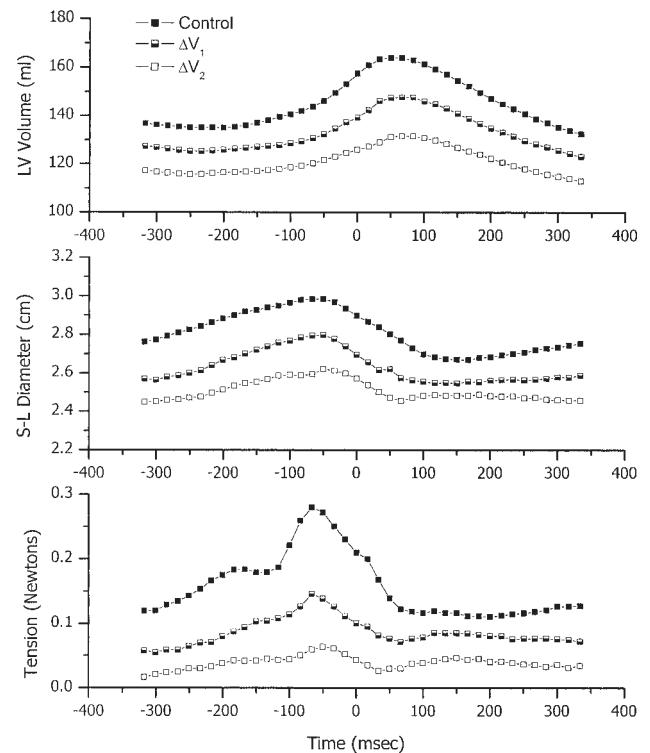


Figure 3: Left ventricular volume (top panel), septal-lateral mitral annular diameter (middle panel), and suture tension (bottom panel) throughout the cardiac cycle at baseline (solid squares) and during two progressive stages of abrupt preload reduction (half-solid [ΔV_1] and open [ΔV_2]). A 650-ms time interval centered at end-diastole ($t = 0$) is illustrated for all three conditions.

Results

The mean total CPB time was 82 ± 9 min, and the mean aortic cross-clamp time 61 ± 7 min. Correct marker positioning and integrity of the leaflet-approximating stitch were confirmed in all animals at post-mortem examination.

Volume occlusion

Hemodynamic variables at baseline and during two volume reduction steps are summarized in Table I. As expected, peak and end-diastolic left ventricular pressure (LVP), EDV and stroke volume were all decreased significantly during each occlusion step compared with baseline. The heart rate did not change. The relationship between LV volume, annular SL diameter and Alfieri stitch (transducer) tension throughout the cardiac cycle at baseline and during volume reduction is shown in Figure 3. Maximum LV volume (165 ± 31 ml, 148 ± 34 ml and 132 ± 36 ml for baseline, $\Delta V1$ and $\Delta V2$, respectively; $p = 0.005$ by ANOVA), SL diameter (3.03 ± 0.32 cm, 2.84 ± 0.37 cm and 2.69 ± 0.41 cm for baseline, $\Delta V1$ and $\Delta V2$, respectively; $p = 0.0005$ by ANOVA), and transducer tension (0.30 ± 0.18 N, 0.18 ± 0.12 N and 0.09 ± 0.06 N for baseline, $\Delta V1$ and $\Delta V2$, respectively; $p = 0.0005$ by ANOVA) decreased significantly during each preload reduction step. At baseline, peak transducer tension was observed at 96 ± 61 ms prior to end-diastole coincident with peak annular SL diameter (98 ± 58 ms before end-diastole), which was significantly earlier than the time of maximum LV volume (54 ± 17 ms after end-diastole; $p = 0.004$ versus time of peak tension). The maximal MAA at baseline was 9.1 ± 1.4 cm² in late diastole (75 ± 44 ms prior to end-diastole).

Dobutamine infusion

In order to investigate the effects of inotropic stimulation and augmented systolic pressure on Alfieri stitch tension, transducer tension, annular SL diameter and LVP were calculated throughout the cardiac cycle

during dobutamine infusion (Fig. 4.) With dobutamine, the heart rate (115 ± 18 versus 86 ± 17 bpm; $p = 0.02$), peak LVP (138 ± 19 versus 115 ± 14 mmHg; $p = 0.03$) and LV dP/dt ($3,382 \pm 624$ versus $1,589 \pm 572$ mmHg/s; $p = 0.004$) were all increased relative to baseline, while LV ESV fell (106 ± 28 versus 128 ± 33 ml; $p = 0.004$). The maximum SL diameter was decreased from 3.03 ± 0.32 cm at baseline to 2.89 ± 0.36 cm with dobutamine infusion ($p = 0.03$), while peak transducer tension fell from 0.30 ± 0.18 N to 0.20 ± 0.12 N ($p = 0.01$). Again, the temporal change in tension closely followed the change in SL diameter, with LV systolic pressure having little effect. Indeed, both at baseline and during inotropic stimulation, Alfieri stitch tension was falling during early systole while LVP was rising abruptly. At the time of peak LVP, both SL diameter and stitch tension were near minimum.

Predictors of Alfieri stitch tension

Six hemodynamic and geometric variables (ranges in parentheses) were used as candidate predictors of suture tension, and included LVP (3 to 193 mmHg), LV dP/dt ($-1,976$ to $3,652$ mmHg/s), LV volume (74 to 217 ml), MAA (4.5 to 10.9 cm²), mitral annular septal-lateral dimension (1.9 to 3.5 cm), and mitral annular commissure-commissure dimension (2.6 to 4.5 cm). Two stages of statistical analysis were used to determine the predictors of Alfieri stitch tension. The first stage is known as 'time-warping'. Initially, there were 32 different observation curves, with eight animals being studied under four conditions (baseline, $\Delta V1$, $\Delta V2$ and dobutamine). Each had a different time scale, depending on the characteristics of the cardiac cycle (e.g., heart rate, amount of time spent in diastole). In order to synchronize the different curves, the time scale was adjusted to make their LVP move roughly in parallel. Thus, a universal time scale was created for the different curves (20). Once the heart cycles had a comparable time scale, it was possible to use a more appropriate regression technique. In ordinary linear

Table I: Hemodynamics.

Parameter	Baseline	$\Delta V1$	$\Delta V2$	p-value (ANOVA)
HR (bpm)	86 ± 17	92 ± 24	91 ± 24	0.5
LVPmax (mmHg)	115 ± 14	$106 \pm 11^*$	$90 \pm 10^*$	0.0005
dP/dt (mmHg/s)	$1,589 \pm 585$	$1,558 \pm 572$	$1,322 \pm 424^*$	0.002
LVEDP (mmHg)	19 ± 7	$12 \pm 5^*$	$8 \pm 3^*$	0.0005
EDV (ml)	158 ± 32	$142 \pm 33^*$	$128 \pm 35^*$	0.0005
SV	30 ± 14	$22 \pm 9^*$	$17 \pm 6^*$	0/.001

* $p < 0.025$ versus baseline by *t*-test for paired comparisons.

dP/dt: Maximum positive rate of change of left ventricular pressure; EDV: Left ventricular end-diastolic volume; HR: Heart rate; LVEDP: Left ventricular end-diastolic pressure; LVPmax: Maximum LV pressure; SV: Stroke volume.

regression, each predictor is assigned a single coefficient; however, for this problem a single coefficient does not suffice, as in different stages of the cardiac cycle a predictor may have a different impact. As an example, high LVP is a predictor for tension during diastole, but during systole the effect is reversed (Fig. 5). Hence, different coefficients are needed for each point in time. The appropriate model was fitted in S-Plus (Mathsoft, Inc., Cambridge, MA, USA) using a periodic least-squares time-varying coefficients model (21). Subsequently, 95% confidence intervals (CI) were generated by bootstrapping the residual tension curves. LVP was the only predictor for which the effect varied significantly with time. Other significant predictors (with 95% CI) were best fit as constant in time, including septal-lateral annular diameter (0.2115 (CI 0.1237, 0.2800)) and MAA divided by septal-lateral diameter (-0.1996 (CI -0.3237, -0.0771)). An intercept term (0.1916 (CI -0.2988, 0.4144)) was also included. In addition, several candidate predictors were not found to be predictive; including LV dP/dt , LV volume and annular commissure-commissure dimension. In this

model, tension at any time (T_t) during the cardiac cycle was described by the mathematical equation:

$$T_t \text{ (N)} = 0.1916 + 0.2115 \times \text{SL (cm)} - 0.1996 \times \text{MAA/SL (cm}^2\text{/cm)} + f_t \times \text{LVP (mmHg)}$$

where SL represents septal-lateral annular diameter, MAA mitral annular area, and f_t the time-varying coefficient of LVP. This model used 28 degrees of freedom to explain 57% of the variance across 1,166 measurements of Alfieri stitch tension.

Discussion

Mitral valve repair is currently the preferred surgical procedure for the correction of mitral insufficiency of various etiologies (1,22,23). The addition of the Alfieri edge-to-edge repair has widened the indications for mitral valve repair according to some investigators (11,12,24). Since the repair approximates the edge of the two mitral leaflets with a single suture, concerns about mitral stenosis and limited durability have arisen. Both clinical (12,13,15) and experimental (16,25) studies have shown that stenosis after the edge-to-edge repair is unlikely, but valve gradients increase significantly with exercise (26). Although good mid-term results have been reported with the Alfieri repair in some forms of mitral pathology (12), the durability of the technique is yet to be firmly established. One determinant of repair durability may be an excessive degree of tension on the approximating suture, but the factors which affect Alfieri stitch tension are not

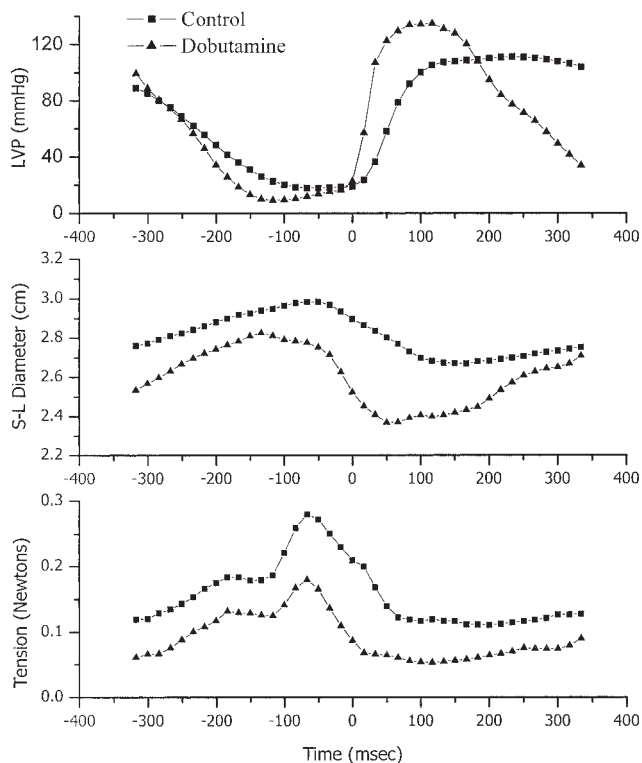


Figure 4: Left ventricular pressure (LVP) (top panel), mitral septal-lateral (S-L) annular diameter (middle panel), and suture tension (bottom panel) throughout the cardiac cycle at baseline (squares) and during inotropic stimulation with dobutamine (triangles). A 650-ms time interval centered at end-diastole ($t = 0$) is illustrated for both conditions.

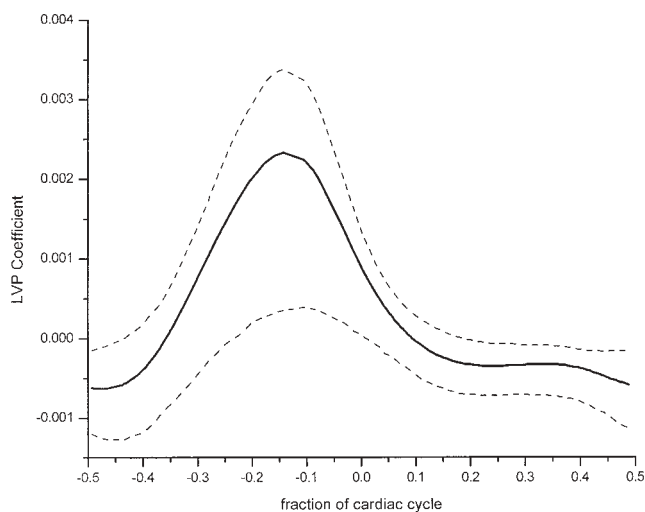


Figure 5: Time varying left ventricular pressure (LVP) coefficient (solid line) throughout the cardiac cycle; 95% confidence limits are illustrated by the dashed lines. The cardiac cycle is centered at end-diastole, with systole to the right and diastole to the left of point zero.

known. In the current study with sheep, a wide range of hemodynamic conditions were created using volume reduction and dobutamine infusion after the mitral leaflets were approximated using a force transducer. Consequently, it was found that tension on the leaflet approximation point was determined mainly by mitral annular size, and the septal-lateral annular diameter in particular.

Maximum suture tension was observed in diastole when annular area and septal-lateral diameter were maximal. Peak tension at baseline was 0.30 ± 0.18 N, which is similar to the tension in primary chordae tendineae reported recently in a porcine in-vivo study (27). This value also agrees closely with the longitudinal stress on the Alfieri stitch of 0.39 N estimated from a 3-D computational model of stress distribution after edge-to-edge repair (28). Systolic tension on the Alfieri stitch was low (and actually approached zero) in early systole and throughout ejection. These observations concur with the clinical predictions of Umaña et al. (13) and the theoretical computational model of Arts et al. (29). Maximal LV volume did not coincide temporally with peak tension under baseline conditions or during two stages of abrupt preload reduction, suggesting that LV chamber size - aside from the its influence on annular size - had little effect on suture tension. Interestingly, during dobutamine infusion, peak systolic pressure increased substantially while both systolic and diastolic suture tension values fell, most likely due to a smaller annular size secondary to inotropic stimulation (30). These findings further suggest that systolic blood pressure does not significantly affect stress on the leaflet-approximating point.

Statistical analysis of the predictors of suture tension, including hemodynamic parameters and valvular dimensions, revealed annular size to be a strong predictor of suture tension. The effect was constant with time throughout the cardiac cycle - that is, annular area and septal-lateral size influence Alfieri stitch tension during both systole and diastole. Interventions or hemodynamic conditions which reduce annular septal-lateral diameter would be expected to reduce suture tension, while those that increase this dimension should increase tension. Indeed, dilation of annular septal-lateral diameter during acute ischemia has been shown to increase stitch tension significantly (31). Computational analysis of stress distribution on the leaflet approximation point after the double-orifice repair revealed a 253% increase in longitudinal stress on the Alfieri stitch after only a 20% increase in annular area (28). Conversely, a reduction of annular septal-lateral dimension through either complete (32) or partial (33) ring annuloplasty should reduce suture tension, as postulated by Arts et al. (29), though this assumption remains to be proven clinically. Currently,

advocates of the Alfieri mitral valve technique usually add concomitant ring annuloplasty (9,11); such annular reduction may decrease suture tension as the annular septal-lateral dimension is substantially smaller. McCarthy et al. (15) performed the Alfieri repair without ring annuloplasty in four patients undergoing partial left ventriculectomy, and all developed substantial mitral insufficiency within several months, possibly due to progressive annular dilatation and excessive stitch tension (as annular dilation in cardiomyopathy develops mainly in the septal-lateral dimension) (34). An undersized (26 mm) Cosgrove-Edwards ring was implanted in subsequent patients, and this resulted in a more durable repair. Furthermore, Lorusso et al. (35) reported that severe atrial dilatation and the use of pericardial annuloplasty as opposed to ring annuloplasty were significant predictors of operative failure in the edge-to-edge technique. These data suggest that annular dilatation probably is associated with poor long-term results after an Alfieri repair, especially as atrial and annular dynamics are closely linked (36,37). In the largest clinical series of edge-to-edge mitral repairs, Alfieri et al. (38) reported that a lack of concomitant annuloplasty was an independent risk factor for reoperation in a multivariable logistic regression analysis. In a recent analysis of 91 patients who underwent the edge-to-edge mitral repair without a ring annuloplasty, Maisano et al. (39) observed suboptimal clinical results, especially in patients with annular calcification. Thus, it appears that concomitant ring annuloplasty is needed. Although it is attractive to speculate that an annuloplasty reduces annular septal-lateral diameter and consequently reduces Alfieri stitch tension, such conclusions at this time cannot be supported on clinical grounds. Annular reduction may decrease suture tension by making the septal-lateral dimension smaller, but this may not guarantee long-term Alfieri repair durability.

The two other predictors of suture tension were mitral annular area divided by septal-lateral diameter and LVP. The ratio of annular area to septal-lateral diameter had an inverse predictive effect which was constant throughout the cardiac cycle. Thus, mitral annular shape, as represented by this relationship, appears to have an important effect on suture tension. The commissure-commissure diameter was not a significant predictor of suture tension, even though the ratio of MAA/SL partially reflects this annular dimension. The normal ratio of annular septal-lateral to commissure-commissure diameters in the human mitral valve (40) is approximately 3:4, and this has also been confirmed in the ovine valve (41). A more circular valvular shape has been associated with mitral regurgitation in acute posterolateral LV ischemia (42) and tachycardia-induced cardiomyopathy (34), whereas

commissure-commissure dilatation does not appear to lead to mitral regurgitation (43). Thus, a less circular valve orifice would be expected to reduce the tension on the approximating stitch in the edge-to-edge repair, though whether this is a reflection of smaller annular septal-lateral diameter or is indicative of better overall stress distribution of this valvular configuration is not known. The LVP coefficient was the only predictor of suture tension which varied with time during the cardiac cycle; it had only a small effect during systole, indicating that systolic blood pressure is not a major determinant of Alfieri stitch tension. LVP had a greater effect in late diastole, when suture tension was maximal, but the coefficient was small. In the context of clinical heart failure, however, a high diastolic LVP could contribute importantly to suture tension.

In the present experiment, predictors of Alfieri stitch tension were identified in an acute, open-chest sheep preparation using a miniature force transducer to approximate the central edge of the mitral leaflets. Peak suture tension was observed during late diastole, and subsequently fell almost to zero during systole. The annular septal-lateral dimension was the major determinant of suture tension, in addition to mitral annular shape; systolic LVP had only a small effect. Mitral procedures which reduce mitral annular size or prevent annular septal-lateral dilatation may therefore be expected to reduce suture tension and perhaps improve durability of the edge-to-edge repair, though whether this will be borne out in the clinical arena remains to be investigated.

Study limitations

The major limitations of the present study were inherent to the animal model. The tension measurements were obtained in sheep which were anesthetized and studied under open-chest conditions, and no annuloplasty rings were used, thereby limiting extrapolation of the experimental results to the human situation. Because of a desire to study the effect of annular size on Alfieri stitch tension, ring annuloplasty was not included in the surgical procedure, as annuloplasty rings - whether flexible or rigid - abolish mitral annular dynamics (32). The surgical procedure necessitated implantation of small metallic markers around the mitral annulus, and this could in theory affect normal annular motion. However, echocardiographic studies indicated that the markers did not interfere with mitral annular or leaflet motion as they were very small (aggregate mass 20 ± 6 mg). Although annular size affects Alfieri stitch tension, and annular dilatation (especially in the septal-lateral dimension) increases suture tension, it is yet not known what effect an increased suture tension might have on the durability of an edge-to-edge repair. The present study inves-

tigated Alfieri stitch tension with approximation of the central edges of both leaflets, but whether the present findings would be applicable if an 'asymmetric' double-orifice repair were to be performed (i.e., with the suture placed towards either commissure) is not known.

Acknowledgements

The authors are appreciative of the superb technical assistance provided by Mary K. Zasio BA, Carol W. Mead BA, and Maggie Brophy AS. These studies were supported by Grants HL-29589 and HL-67025 from the National Heart, Lung and Blood Institute. Drs. T. A. Timek, D. T. Lai and F. Tibayan are Carl and Leah McConnell Cardiovascular Surgical Research Fellows. Dr. Timek is a recipient of the Thoracic Surgery Foundation Research Fellowship Award. Dr. Nielsen was supported by grants from the Danish Heart Foundation. Drs. Timek and Tibayan were also supported by NHLBI INRSA HL-10452 and HL-67563, respectively. Dr. Lai was supported by a fellowship from the American Heart Association, Western States Affiliate.

References

1. Deloche A, Jebara VA, Relland JY, et al. Valve repair with Carpentier techniques. The second decade. *J Thorac Cardiovasc Surg* 1990;99:990-1001
2. Reul RM, Cohn LH. Mitral valve reconstruction for mitral insufficiency. *Prog Cardiovasc Dis* 1997;39:567-599
3. Enriquez-Sarano M, Schaff HV, Orszulak TA, et al. Valve repair improves the outcome of surgery for mitral regurgitation. A multivariate analysis. *Circulation* 1995;91:1022-1028
4. Carpentier A. Cardiac valve surgery - the 'French correction'. *J Thorac Cardiovasc Surg* 1983;86:323-337
5. Uva MS, Jebara V, Fuzelier JF, et al. Transposition of chordae in mitral valve repair. *Circulation* 1993;88:35-38
6. Bernal JM, Rabasa JM, Olalla JJ, Carrion MF, Alonso A, Revuelta JM. Repair of chordae tendineae for rheumatic mitral valve disease. A twenty-year experience. *J Thorac Cardiovasc Surg* 1996;111:211-217
7. David TE, Omran A, Armstrong S, Sun Z, Ivanov J. Long-term results of mitral valve repair for myxomatous disease with and without chordal replacement with expanded polytetrafluoroethylene sutures. *J Thorac Cardiovasc Surg* 1998;115:1279-1285
8. Dreyfus G, Al Ayle N, Dubois C, de Lentdecker P. Long term results of mitral valve repair: posterior papillary muscle repositioning versus chordal

- shortening. *Eur J Cardiothorac Surg* 1999;16:81-87
9. Fucci C, Sandrelli L, Pardini A, Torracca L, Ferrari M, Alfieri O. Improved results with mitral valve repair using new surgical techniques. *Eur J Cardiothorac Surg* 1995;9:621-626
 10. Maisano F, Torracca L, Oppizzi M, et al. The edge-to-edge technique: A simplified method to correct mitral insufficiency. *Eur J Cardiothorac Surg* 1998;13:240-245
 11. Maisano F, Schreuder JJ, Oppizzi M, Fiorani B, Fino C, Alfieri O. The double-orifice technique as a standardized approach to treat mitral regurgitation due to severe myxomatous disease: Surgical technique. *Eur J Cardiothorac Surg* 2000;17:201-205
 12. Totaro P, Tulumello E, Fellini P, et al. Mitral valve repair for isolated prolapse of the anterior leaflet: An 11-year follow-up. *Eur J Cardiothorac Surg* 1999;15:119-126
 13. Umaña JP, Salehizadeh B, DeRose JJ, Jr., et al. 'Bow-tie' mitral valve repair: An adjuvant technique for ischemic mitral regurgitation. *Ann Thorac Surg* 1998;66:1640-1646
 14. Batista RJ, Verde J, Nery P, et al. Partial left ventriculectomy to treat end-stage heart disease. *Ann Thorac Surg* 1997;64:634-638
 15. McCarthy PM, Wong J, Scalia GM, et al. Early results with partial left ventriculectomy. *J Thorac Cardiovasc Surg* 1997;114:755-765
 16. Timek TA, Liang D, Lai DT, et al. Edge-to-edge mitral repair: gradients and three-dimensional annular dynamics in vivo during inotropic stimulation. *Eur J Cardiothorac Surg* 2001;19:431-437
 17. Nielsen SL, Nygaard H, Fontaine AA, et al. Chordal force distribution determines systolic mitral leaflet configuration and severity of functional mitral regurgitation. *J Am Coll Cardiol* 1999;33:843-53
 18. Daughters GT, Stewart W, Miller DC, Schwartzkopf A, Mead CW, Ingels NB. A comparison of two analytical systems for three-dimensional reconstruction from biplane videoradiograms. *Proc Comp Cardiol (IEEE)* 1988;15:79-82
 19. Moon MR, DeAnda A, Daughters GT, Ingels NB, Miller DC. Experimental evaluation of different chordal preservation methods during mitral valve replacement. *Ann Thorac Surg* 1994;58:931-944
 20. Kneip A LK, MacGibbon KB, Ramsay JO. Curve registration by local regression. *Can J Statist* 2000;28:19-30
 21. Hastie TTR. Varying coefficients models. *J Royal Statist Soc (Series B)* 1993;55:757-796
 22. Akins CW, Hilgenberg AD, Buckley MJ, et al. Mitral valve reconstruction versus replacement for degenerative or ischemic mitral regurgitation. *Ann Thorac Surg* 1994;58:668-675
 23. Bernal JM, Rabasa JM, Vilchez FG, Cagigas JC, Revuelta JM. Mitral valve repair in rheumatic disease. The flexible solution. *Circulation* 1993;88:1746-1753
 24. Maisano F, Torracca L, Oppizzi M, et al. The edge-to-edge technique: A simplified method to correct mitral insufficiency. *Eur J Cardiothorac Surg* 1998;13:240-246
 25. Maisano F, Redaelli A, Pennati G, Fumero R, Torracca L, Alfieri O. The hemodynamic effects of double-orifice valve repair for mitral regurgitation: A 3D computational model. *Eur J Cardiothorac Surg* 1999;15:419-425
 26. Borghetti CM, Scotti C, Parrinello G, Lorusso R. Preliminary observations on hemodynamics during physiological stress conditions following 'double-orifice' mitral valve repair. *Eur J Cardiothorac Surg* 2001;20:262-268
 27. Lomholt NS, Hansen SB, Andersen NT, Hasenkam JM. Differential tension between secondary and primary mitral chordae in an acute in-vivo porcine model. *J Heart Valve Dis* 2002;11:337-345
 28. Votta E, Sonicini R, Redaelli A, Montevecchi FM, Alfieri O. 3-D computational analysis of the stress distribution on the leaflets after edge-to edge repair of mitral regurgitation. *J Heart Valve Dis* 2002;11:810-822
 29. Arts T, Meerbaum S, Reneman R, Corday E. Stresses in the closed mitral valve: A model study. *J Biomech* 1983;16:539-547
 30. Gorman JH, Jackson BM, Kelley ST, Melekan R, Edmunds LH, Jr. Effect of inotropic state on the size of the mitral valve annulus. *Surg Forum* 1997;48:275-278
 31. Nielsen SL, Timek TA, Lai DT, et al. Edge-to-edge mitral repair: Tension on the approximating suture and leaflet deformation during acute ischemic mitral regurgitation in the ovine heart. *Circulation* 2001;104(suppl.1):I-29-I-35
 32. Glasson JR, Green GR, Nistal JF, et al. Mitral annular size and shape in sheep with annuloplasty rings. *J Thorac Cardiovasc Surg* 1999;117:302-309
 33. Dagum P, Timek TA, Green GR, et al. Three dimensional geometric comparison of partial and complete flexible mitral annuloplasty rings. *J Thorac Cardiovasc Surg* 2001;122:665-673
 34. Timek TA, Dagum P, Lai DT, et al. Pathogenesis of mitral regurgitation in tachycardia induced cardiomyopathy. *Circulation* 2001;104(suppl.1):I-47-I-53
 35. Lorusso R, Totaro P, Parrinello G, Coletti G, Minzioni G. The double-orifice technique for mitral valve reconstruction: Predictors of postoperative outcome. *Eur J Cardiothorac Surg* 2001;20:583-589
 36. Timek TA, Lai D, Tibayan FA, et al. Atrial contraction and mitral annular dynamics during acute left

- atrial and ventricular ischemia in sheep. *Am J Physiol* 2002;283:H1929-1935
37. Timek TA, Dagum P, Lai DT, et al. The role of atrial contraction in mitral valve closure. *J Heart Valve Dis* 2001;10:312-319
 38. Alfieri O, Maisano F, De Bonis M, Stefano PL, Torracca L, Oppizzi M. The double-orifice technique in mitral valve repair: A simple solution for complex problems. *J Thorac Cardiovasc Surg* 2001;122:674-681
 39. Maisano F, Blasio A, De Bonis M, et al. Mid-term results of the edge-to-edge mitral valve repair without annuloplasty. Annual Meeting of the American Association for Thoracic Surgery, May 4-7, 2003, Boston, Massachusetts. Abstract
 40. Carpentier AF, Lessana A, Relland JY, et al. The 'physio-ring': An advanced concept in mitral valve annuloplasty. *Ann Thorac Surg* 1995;60:1177-1185
 41. Glasson JR, Komeda M, Daughters GT, et al. Most ovine mitral annular 3-D size reduction occurs before ventricular systole and is abolished with ventricular pacing. *Circulation* 1997;96:II-115-II-123
 42. Glasson JR, Komeda M, Daughters GT, et al. Early systolic mitral leaflet 'loitering' during acute ischemic mitral regurgitation. *J Thorac Cardiovasc Surg* 1998;116:193-205
 43. Green GR, Dagum P, Glasson JR, et al. Mitral annular dilatation and papillary muscle dislocation without mitral regurgitation in sheep. *Circulation* 1999;100:II-95-II-102